MRS Advances © 2018 Materials Research Society
DOI: 10.1557/adv.2018.244

Gd – Gd_2O_3 multimodal nanoparticles as labeling agents

Pedro Perdigon-Lagunes[1*], Octavio Estevez[1], Cristina Zorrilla Cangas[1], Raul Herrera-Becerra[1]

[1]*Universidad Nacional Autonoma de Mexico (UNAM), Instituto de Fisica, Mexico City, CDMX, Mexico*
**pedroperdigon@estudiantes.fisica.unam.mx*

ABSTRACT

Lanthanide nanoparticles had the possibility to couple many imaging techniques into a sole labeling agent has awaken high expectations on personalized medicine or <<Theranostics>>. This is possible due to their intrinsic physic – chemical properties. Combining different imaging techniques physicians may provide a better treatment and perform surgical procedures that might increase the survival rate of patients. Hence, there is an enormous opportunity area for the development of lanthanide multimodal nanoparticles. For this study, we synthesized Gd – Gd_2O_3 nanoparticles at room temperature by reduction method assisted by Tannic acid, and later we doped them with different ratios of Eu. The nanoparticles were analyzed through high resolution microscopy (HRTEM), Raman Spectroscopy, luminescence, and magnetic characterizations. We found small nanoparticles with a mean size of 5 nm, covered in a carbonaceous layer. In addition, different emissions were detected depending on Eu concentration. Finally, the magnetization vs. temperature recorded under zero field cooled (ZFC) and field cooled (FC) conditions exhibit an antiferromagnetic to ferromagnetic phase transition in samples with Gd_2O_3, and hysteresis loops recorded at 100 Oe and 2 K showed a relevant magnetization without magnetic remanence. Hence, these nanomaterials have interesting properties to be tested in biocompatibility assays.

I INTRODUCTION

Lanthanide nanoparticles have captured the attention in many fields, such as energy conversion, sustainability, electronics, photonics and biomedicine.[1-5] The promise of coupling many imaging techniques into a sole labeling agent has awaken high expectations on personalized medicine or <<Theranostics>>.[4,6,7]

Magnetic resonance imaging (MRI) treatments offer the opportunity to detect in a non – invasive form of cancerous formations with the help of labeling agents such as SPIONs,[8,9] Gd^{3+} chelates,[10] and Gd – based nanoparticles.[7,11,12] However, lanthanide based nanoparticles are able to fuse other techniques due to their intrinsic physic – chemical properties. Combining different techniques such as MRI/Endoscopy, computerized tomography (CT)/Positron emission tomography (PET), CT/MRI, and Endoscopy/CT might provide a better treatment approach for hidden diseases as cancerous tumors. In addition, an interesting aspect of using these types of labeling agents is the opportunity to perform surgical procedures in situ; this gives the possibility of detecting and acting at the same time, increasing the survival rate of the patients.

Therefore, we identified an opportunity area for the development of lanthanide multimodal nanoparticles. For this study, we synthesized Gd – Gd_2O_3 nanoparticles at room temperature by reduction method assisted by Tannic acid. Owing to the chemistry of lanthanides, other nanoparticles were also tested in comparison: EuO, GdEu alloy, and Gd doped in 5% with Eu (Gd@Eu), all synthetized with the same method. Then, we analyzed nanoparticles through HRTEM, Raman Spectroscopy, luminescence, and magnetic characterizations. With these studies, we may understand the potential of these nanoparticles as multimodal labeling agents for biomedicine.

II SYNTHESIS AND CHARACTERIZATION

The nanoparticles were synthesized through reduction reaction using tannic acid as reduction agent.[13-15] A similar method was used to synthesize different lanthanide nanoparticles;[3,16-19] however, for this case we used synthetic tannin instead of plants, with similar results.

To synthetize the Gd – Gd_2O_3, EuO and Eu doped Gd nanoparticles for each lanthanide a 3mM dissolution of $Gd(NO_3)_3 \cdot 6\,H_2O$ (Sigma Aldrich MW 451.36 99.999%) and $Eu(NO_3)_3 \cdot 5\,H_2O$ (Sigma Aldrich MW 428.06 99.9% trace metals) was prepared in 15 ml of deionized water and a dissolution of 0.045 mM of Tannic acid ($C_{76}H_{52}O_{46}$) (Sigma Aldrich MW 1701.20 Zn ≤ 0.005% Heavy metals ≤ 0.003 %) also in 15 ml of deionized water was prepared. In addition, a 0.1 M dissolution of NaOH (J.T. Baker MW 40.00 98.4%) in 5 ml of deionized water was prepared to regulate the pH of the synthesis. On constant stirring, 15 ml of $Gd(NO_3)_3 \cdot 6\,H_2O$ dissolution were added with 15 ml

of Tannic acid for Gd – Gd_2O_3; in the case of EuO 15 ml of $Eu(NO_3)_3 \cdot 5\ H_2O$, were used with 15 ml of Tannic acid. For hybrid nanoparticles Gd was replaced with Eu dissolution in 50% for GdEu and 5% for Gd@Eu. Then, each dissolution was added NaOH dissolution until they reached pH 11 and sonicated for 5 minutes with the intention of activating all the clustering sites. Then to stop the growth of the nanoparticles, the dissolution was frozen into liquid nitrogen and finally was lyophilized until it dried.

TEM micrographies were taken on a JEOL JEM-2010F FasTem a 200 keV, and a fast Fourier transform (FFT) was performed over a HRTEM micrographie using Gatan 3.7.0 software to obtain structural information.[20] Raman spectra were taken in a Thermo Scientific DXR Raman Microscope device with a 633 nm laser excitation, to avoid fluorescence. Luminescence spectra were taken in a Pelking Elmer device with a 290 nm excitation in a quartz cell. Magnetic measurements were taken in a SQUID device model MPMS3.

III RESULTS AND DISCUSSION

a. Nanoparticles characterization

TEM microscopy

In Figure 1 a nanoparticle matrix made from tannic acid was observed, with an approximate size of 30 nm. This structure engulfed our nanoparticles. From figure 1 we obtained their size, their diameter varies from 2 to 8 nm. Thus, they might be candidates for biomedicine due to its dimensions. The nanoparticles had a compact crystalline – like structure, similar to truncated cuboctahedrons. Figure 1 also shows as an insert a HRTEM image from one of these nanoparticles, and this one was used to obtain crystallographic information through a FFT. In this case, the reflections were compared to crystalographic bases using our software to determine the crystaline like structure. [21-23] The analysis indicated the presence of β - Gd and C – Gd_2O_3 phases.

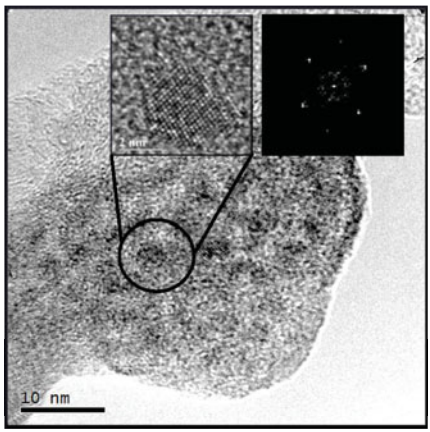

Figure 1: Gd-Gd2O3 nanoparticles are engulfed by a tannin the mean size is 5 nm. As an insert, a HRTEM nanoparticle was taken; then, a FFT was performed to obtain structural information.

Using these Gd – Gd_2O_3 nanoparticles as a starting point, we decided to dope these nanomaterials with Eu^{3+} in different proportions: 5% (Gd@Eu) and 50% (GdEu); in addition, we made a 100% EuO nanoparticle; on each case, we obtained Gd/Eu – oxide nanoparticles. Structurally, all the nanoparticles presented a similar shape and crystalline – like assembly. Nevertheless, other techniques were necessary to determine the type of oxide presented on each sample.

Raman spectroscopy

Figure 2 shows the Raman spectra taken over the lanthanide nanoparticles, some fluorescence emission persisted. In 180 cm^{-1} a clear bound between Gd or Eu with O was revealed. Gd and Eu had similar Raman response, both had the C-type rare earth oxide structure. [24] On each case, we found the same structure which indicated that both materials were similarly self – ensembled.[25] In addition, we identified an organic layer at 720 and 1382 cm^{-1} firmly attached over the nanoparticles.

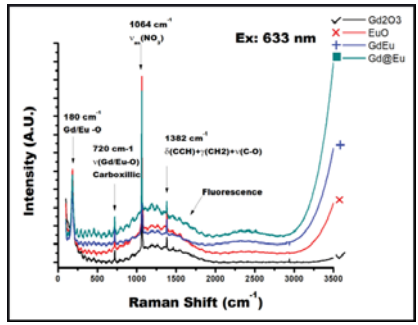

Figure 2: Raman spectra of lanthanide nanoparticles. On each case, similar structure was found. At 180 cm^{-1} and 720 cm^{-1} O – Gd/Eu interactions were present. A strong presence of carbonaceous cover was also revealed at 1382 cm^{-1}. A strong fluorescent component interfered with the spectra.

This interaction was clearly observable at Figure 1, where the nanoparticles were engulfed into an organic layer with a high density of nanoparticles, which might lead to increase the biocompatibility.[10] Therefore, microscopy and Raman results indicated the high efficacy of self – ensembled small nanoparticles with structure similar to bixbyite covered with a carbonaceous layer. As consequence of the bixbyite type structure, the lanthanides may behave as Gd^{3+} and Eu^{3+}; hence, they should present interesting optical and magnetic properties. This was reflected on the luminescence effect observed at the Raman spectra.

b. Nanoparticles optic and magnetic properties

Luminescence

In this case (Figure 3), different behaviors were found. In Gd_2O_3, EuO and GdEu samples the same emission in 417 nm was revealed, this corresponded to UV lanthanide excitation; however, in Gd@Eu the emission was displaced to 430 nm. This may indicate a special coupling between Gd and Eu. Another interesting result was found only in EuO. This sample presented peculiar emissions, at 354 and 685 nm. In the literature, [26] emission from Gd_2O_3:Eu corresponded mostly to a transition $^5D_0$ to $^7F_1$ that depended on the excitation of Eu^{3+} ions that doped Gd_2O_3. Due to its structure, we expected to find Eu^{3+} emissions; nevertheless, in our results we found a mayor presence of Eu^{2+} over Eu^{3+}, this result was unexpected.

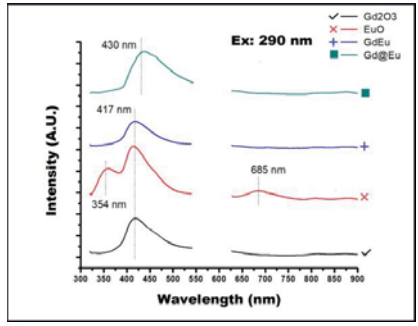

Figure 3: Luminescence spectra of lanthanide nanoparticles. Depending on the composition of the nanoparticles, different emissions were localized. Interestingly, in all cases Gd^{3+} or Eu^{3+} were present but in Eu oxide. In that case the emissions corresponded to Eu^{2+}.

In figure 3 we observed Gd@Eu nanoparticles did not behave as expected. In this case, Eu^{2+} emission was observed, instead of Eu^{3+}. A possible explanation is a symmetry break over the nanoparticle surface, where more oxygen was present. Consequently, to stabilize the nanoparticle Eu acquires a «3+» valence, while inside the nanoparticle the oxygen was less abundant, then it stabilized at «2+».

Therefore, in this case Gd@Eu may be formed as a composition of different valences. As a consequence, Gd@Eu might not correspond to Gd_2O_3:Eu. This was also present in the sample EuO. However, the emission from EuO at 685 nm corresponding to Eu^{3+} was very strong. Thus, more studies are required to understand the composition of these nanoparticles. Hence, this synthesis process might be used to tune the luminescence of lanthanide base nanoparticles just by changing the ratio of Gd – Eu by a reduction process; additionally, it may be possible to tune their oxidation state. Consequently, the optical properties may be modified.

ZFC – FC

In order to understand their magnetic properties, different magnetic studies were performed over the samples. Figure 4 presented ZFC – FC measurements, where Gd_2O_3 and Gd@Eu nanoparticles (figure 4(a) and 4(d)) presented a dual comportment, between 2 K - 25 K both samples reveal a ferromagnetic (FM) comportment, then at 25 K the nanoparticles switched to antiferromagnetic (AFM) behavior. This is clearly appreciable on the sudden changes that the slope presented. [27] EuO (figure 4(b)) showed a paramagnetic behavior, which might correspond to Eu^{2+} ions in the nanoparticle; moreover, an approximate blocking temperature can be depicted from the inflection point in ZFC plot (figure 4(b)) in T (K) vs M (emu/g), [28] in this case corresponding to 175 K. [8] GdEu presented a double transition (figure 4(c)); at 25 K it changes suddenly from FM to AFM, from 25 to 300 K a paramagnetic (PM) – like behavior was depicted. Figure 4(c) also presented an inflection point that might be interpreted as an approximation of a blocking temperature around 175 K. Therefore, it was the best candidate to present superparamagnetism. Nevertheless, a hysteresis was needed to fully reveal the magnetic characteristics of these lanthanide based materials.

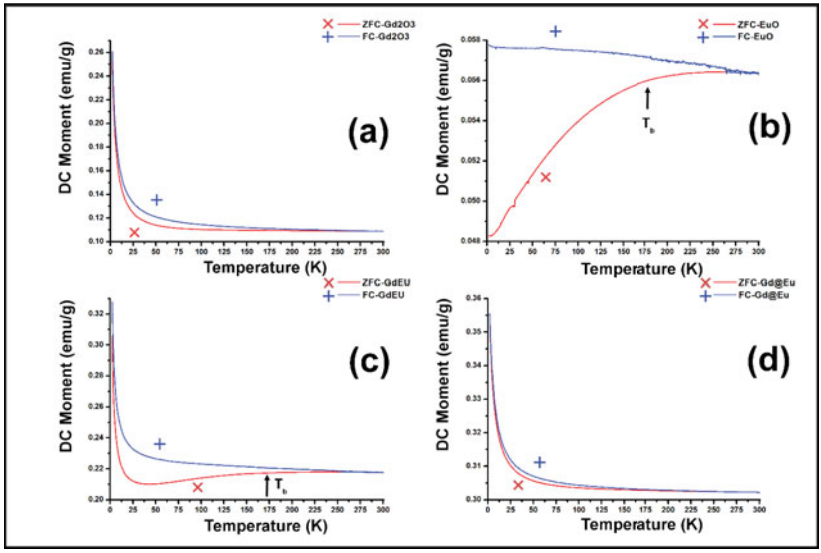

Figure 4: ZFC – FC studies were performed on each sample (a) Gd_2O_3, (b) EuO, (c) GdEu, (d) Gd@Eu. All samples that contained Gd were highly magnetic with a FM – AFM transition; Eu oxide was paramagnetic which indicates the presence of Eu^{2+}; however, the most interesting behavior was depicted at GdEu sample, were a double transition at 35 K was found, this may indicate an AFM transition and a PM behavior over 35 K. In Eu and GdEu samples a blocking temperature (T_b) was possible to approximate as the inflection point in ZFC cycle.

Hysteresis at 2K

Figure 5 shows hysteresis measurements over each sample. In this temperature, the EuO nanoparticles had a diamagnetic contribution. This was because at this temperature EuO nanoparticles did not properly magnetized and it is necessary to increase the temperature up to 175 K to observe a possible superparamagnetic behavior. The other nanoparticles presented a quasi – superparamagnetic comportment. This conduct was probably provoked by a dual phase of Gd – Gd_2O_3 mixture on the nanoparticles. Another interesting result is the difference in magnetization, owing to the increase of the field on GdEu and Gd@Eu. In this case, doping the Gd nanoparticles with 5% of Eu decreases the magnetization in comparison with the GdEu alloy. This may indicate the presence of Eu^{3+} in the Gd@Eu and Eu^{2+} in GdEu, which indicates a strong interaction between both lanthanides. In addition, as an insert in Figure 5 an enlargement around zero field was shown; in this case all nanoparticles did not present any magnetic remanence. This is a consequence of the size of the nanoparticles.

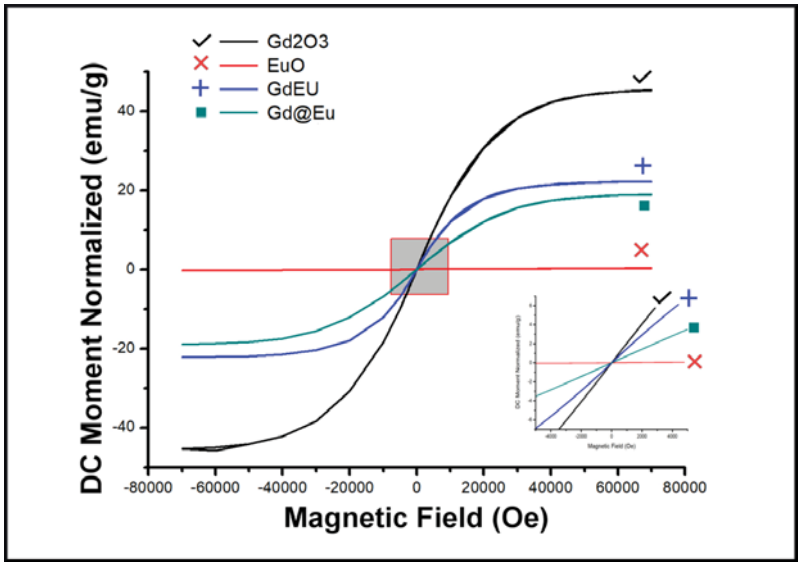

Figure 5: Hysteresis studies at 2 K were performed on each sample. As previously seen at ZFC – FC, all samples that contained Gd were highly magnetizable, Eu oxide was diamagnetic at that temperature. In addition, all nanoparticles with Gd might present superparamagnetic behavior. As an insert, an amplification around 0 Oe demonstrate that these nanoparticles had no magnetic memory to their size.

IV CONCLUSIONS

Lanthanide based nanoparticles were synthetized and tested with different techniques to demonstrate their potential as labeling agents. In this work, we successfully self – ensembled four different lanthanide nanoparticles: Gd – Gd2O3, EuO, GdEu and Gd@Eu. TEM microscopy revealed an enormous population of nanoparticles engulfed by an organic layer, while Raman spectroscopy demonstrated this organic layer is tightly bound to the nanoparticles. In addition, Raman showed the composition and partial structure of the nanoparticles. As a consequence of both techniques, the nanoparticles depicted a promising material to be used in biomedicine. Luminescence and SQUID characterization demonstrated interesting optical and magnetic properties coupled in our nanoparticles, as a consequence of their size, structure and composition. Therefore, our nanomaterials had interesting properties to be tested as optical and magnetic contrast agents for imaging techniques or even multimodal probes, due to the conjunction of magneto-optic attributes. Specially, GdEu and Gd@Eu presented an interesting fusion of properties such as size, luminescence and magnetism; EuO and GdEu presented a possible superparamagnetic behavior, this made them also candidates to be used as agents for hyperthermia. Hence, through our synthesis method, it was possible to obtain hybrid nanoparticles and tune their properties depending on the ratio of lanthanides. This opened the opportunity to generate easy tunable multimodal labeling agents based on lanthanides with applications in biomedicine. However, more work is necessary to tune the nanoparticles and obtain a contrast agent that may also be used as treatment.

ACKNOWLEDGEMENTS

We would like to thank to Roberto Hernandez from IF-UNAM for TEM micrographies and EDX analysis, Antonio Morales and Alejandro Herrera from IF-UNAM for PXRD patterns and analysis, and Maria Cristina Flores from IF-UNAM for the luminescence analysis. We would like to thank to Cristian Sosa-Mosquera and Anna L. Aranda-Poucel for the style and grammar correction. We would also like to thank CONACyT and DGAPA project IN108915 for its economic support.

REFERENCES

1. F. Wang, R. Deng, J. Wang, Q. Wang, Y. Han, H. Zhu, X. Chen and X. Liu, *Nature Materials,* **10**, 968–973 (2011).
2. J. A. Ascencio, A. C. Rincon and G. Canizal, *J. Phys. Chem. B,* **109**, 8806–8812 (2005).
3. J. A. Ascencio, A. Medina-Flores, L. Bejar , L. Tavera, H. Matamoros and H. B. Liu, *J. Nanosci. and Nanotech,* **4**, 1044-1049 (2006).
4. Y. C. Cao, *J. Am.. Chem. Soc.,* **126**, 7456-7457 (2004),.
5. R. Bazzi, M. A. Flores-Gonzalez, C. Louis, K. Lebbou, C. Dujardin, A. Brenier, W. Zhang, O. Tillement, E. Bernstein and P. Perriat, *J. Luminescence,* **102–103**, 445–450 (2003).
6. W. Xu, K. Kattel, Y. Park, Y. Chang, T. J. Kim and G. H. Lee, *Phys. Chem. Chem. Phys,* **14**, 12687–12700 (2012).
7. Z. Shi, K. G. Neoh, E. T. Kang, B. Shuter and S.-C. Wang, *Contrast Media Mol. Imaging,* **5**, 105–111 (2010).
8. M. Tadic, M. Panjan, V. Damnjanovic and I. Milosevic, *Appl. Surf. Sci.,* **320**, 183-187, (2014).
9. C. Rodríguez-Torres, S. Stewart, C. Adán and A. Cabrera, *J. Alloys and Compounds,* **495**, 485–487 (2010).
10. M. Riri, M. Hor, F. Serdaoui and M. Hlaibi, *Arabian Journal of Chemistry*, **2**, S1478–S1486 (2016).
11. M. Norek, G. A. Pereira, C. F. G. C. Geraldes, A. Denkova, W. Zhou and J. A. Peters, *J. Phys. Chem. C,* **111**, 10240-10246 (2007).
12. J. Y. Park, M. J. Baek, E. S. Choi, S. Woo, J. H. Kim, T. J. Kim, J. C. Jung, K. S. Chae, Y. Chang and G. H. Lee, *ACS Nano*, **11**, 3663–3669 (2009).
13. M. Santana-Vázquez, O. Estevez, F. Ascencio-Aguirre, R. Mendoza-Cruz, L. Bazán-Díaz, C. Zorrila and R. Herrera-Becerra, *Appl. Phys. A ,* **122**, 868 1-7 (2016).
14. F. M. Ascencio-Aguirre and R. Herrera-Becerra, *Appl. Phys. A,* **119**, 909–915 (2015).
15. F. M. Ascencio-Aguirre, L. Bazán-Díaz, R. Mendoza-Cruz, M. Santana-Vázquez, O. Ovalle-Encinia, A. Gómez-Rodríguez and R. Herrera-Becerra, *Applied Physics A,* **123**, 155 1-6 (2017).
16. J. A. Ascencio, Y. Mejia, H. B. Liu, C. Angeles and G. Canizal, *Langmuir,* **19**, 5882–5886 (2003).
17. J. A. Ascencio, A. C. Rincon and G. Canizal, *J. Phys. Chem. B,* **109**, 8806–8812 (2005).
18. J. A. Ascencio, A. C. Rodriguez-Monroy, H. B. Liu and G. Canizal, *Chemistry Letters,* **33**, 1056 – 1057 (2004).
19. P. Perdigon-Lagunes, J. A. Ascencio and A. Agarwal, *Appl. Phys. A,* **4**, 2265-2273 (2014).
20. G. S. Team, "Digital Micrograph (TM) **3.7.0** for GMS 1.2," Gatan Inc., Pleasanton, (1999).
21. R. Galicia, R. Herrera, J. Rius, C. Zorrilla and A. Gómez, *Rev. Mex. Fis.,* **59**, 102–106 (2013).
22. I.C. f. D. Data, "Powder Diffraction File, **#12-0797**".
23. I.C. f. D. Data, "Powder Diffraction File, **#65-7936**".
24. W. B. White and V. G. Keramidas, *Spectrochimica Acta,* **28A**, 501-509 (1972).
25. M. V. Abrashev, N. D. Todorov and J. Geshev, *J. Appl. Phys.,* **116**,. 103508 1-7 (2014).
26. N. Dhananjaya, H. Nagabhushana, B. M. Nagabhushana, B. Rudraswamy , C. Shivakumara, K. Narahari and R. P. S. Chakradhar, *S.A.A.,* **86**, 8-14 (2012).
27. A. Mitra, A. S. Mahapatra, A. Mallick, A. Shaw, M. Ghosh and P. K. Chakrabarti, *J. Alloys and Compounds,* **726**, 1195-1204 (2017).
28. B. Martínez, X. Obradors, L. Balcells, A. Rouanet and C. Monty, *Phys. Rev. Lett.,* **1**, 181-184 (1998).